Prediction of Residual Stress States after modified Shot Peening Treatments using Strain-Rate and Temperature-dependent Material Data

A. Klumpp[1], S. Klaus[1], S. Dietrich[1], V. Schulze[1]

1 Institute for Applied Materials (IAM-WK), Karlsruhe Institute of Technology (KIT), Karlsruhe, Germany

Abstract
Within the EU-project “LEAFSLIM”, the application of modified stress peening treatments to leaf springs for heavy truck applications has been investigated. Part of the project was the development of an adequate Finite Element (FE)-simulation model. Using strain-rate and temperature dependent material data, the predictability of residual stresses after conventional, warm, stress, warm stress and double peening was assessed. Both impact analyses and process-oriented simulations were carried out. The simulation framework shows a good reproducibility of experimentally measured residual stress states and tendencies regarding pre-stress and temperature.

Keywords Modified stress peening, leaf springs, surface layer states, FE-simulation

Introduction

During the last decades, numerical simulations have become a versatile and powerful means to predict, investigate and understand the shot peening process and the hereby generated surface states, determined by measures such as residual stress and roughness, cold work and phase composition. Meanwhile, the efforts undertaken in a large number of original investigations have been summarized in exhaustive literature reviews [1,2], giving an overview about the efforts undertaken in the field. Investigations have focused on feasible model assumptions and simplifications regarding particle dynamics, material behavior of target and shot, boundary conditions, friction, among other aspects, within 2D and 3D micro and macro Finite Element (FE)-simulations [1,2]. Within recent years, a trend towards realistic process models has been recognizable, for instance the model of Gariépy et al. [3] which incorporates the random nature of size and velocity distribution of the shots.

One challenging aspect of shot peening simulation has been the target material modeling. Shot peening causes plastic material deformation at very high strain rates, possibly above 10^5/s [4], causing adiabatic heating and evoking mechanisms relevant to high strain rate deformation such as thermally activated dislocation glide and damping effects [5]. Moreover, the multiaxial Bauschinger effect comes into play, since plastic deformation is confined to very small distances from the target surface and multiple shot impacts cause three-dimensional elastic-plastic strain reversals. Various material-related effects have therefore been incorporated in shot peening simulation, giving rise to different approaches such as complex viscoplastic models with combined kinematic and isotropic hardening rules [4,6,7]. One model presented in the past is the thermal activation continuum flow stress model of Voyiadjis & Abed [6] which was adopted to shot peening simulations by Klemenz et al. [7]. Since this type of model is strain-rate and temperature dependent, its application to shot peening at different temperatures, such as warm peening, a common shot peening variant, would be of high interest. Yet, simulations of shot peening variants are very rare. Besides warm peening, typical shot peening variants are stress peening and double peening, all of which are processes highly relevant to the steel spring industry [8].

Warm peening is a modified shot peening process mostly used on steels, during which the work piece exhibits a temperature usually in the range from 170 °C to 350 °C. Due to static and dynamic strain ageing effects, more stable residual stress states can be achieved [8]. Stress peening is a modified shot peening process in which mechanical pre-stress of the

same direction and sign as the future operational load is applied to the work piece during the surface treatment. After unloading from the pre-stress, the shot peening residual stresses are superposed by the reversed bending stresses and therefore of higher magnitude and penetration depth than after conventional peening [8]. Double peening denotes successively applied shot peening processes with different parameters. Peening with coarse and subsequently with fine shot can favorably be used for surface roughness reduction and individual shot peening variants are theoretically combinable to complex peening operations, such as warm stress double peening [9].
Within the EU-project “LEAFSLIM”, the application of such enhanced shot peening variants has been assessed in the context of leaf springs in heavy truck applications (more details in [10,11]). As part of the project, this study aims at presenting an approach toward the simulation of the applied shot peening variants. Besides general tendencies predicted in warm, stress and double peening, some comparisons to experimental data will be shown and subsequently be discussed with regard to other results from the literature.

Experimental and Numerical Methods
The low-alloyed spring steel 51CrV4AR (52CrV4Mo) Q+T was used for the investigation. A detailed description of material and heat treatment can be found in [10].
Shot peening was simulated by means of Finite Element (FE)-Analysis. The FE geometry and mesh were modeled using parameterization. After preliminary mesh convergence and size analyses, a 4*4*4 mm^3 sized cuboid consisting of approx. 200,000 hexahedron elements of type C3D8R was used as simulation model and is shown in Figure 1 (a).

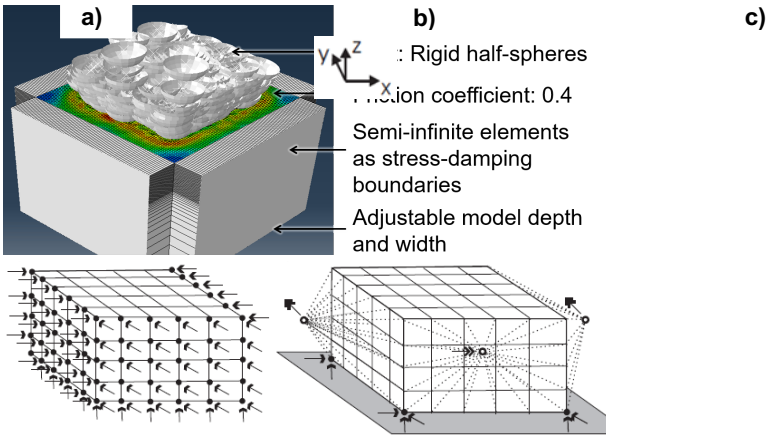

Figure 1. Shot peening simulation model (a); symmetry cell boundary condition (b); kinematic constraint boundary condition (c) [6, 13].

Shots were modeled as analytical rigid half spheres. For the sake of simplicity, mean values of shot velocity and size were assumed using literature data [12]. Shot velocities varying between 20 m/s and 120 m/s were adopted. Since S330 and S170 shots were used in experimental investigations [10,11], the diameters of half spheres in simulation were 0.80 and 0.36 mm, respectively. A friction coefficient of 0.4 between shots and target was used. Semi-infinite elements (CIN3D8) were applied at the laterals to dampen stress waves. Figure 1 (b) and (c) show the applied boundary conditions, namely the symmetry cell and kinematic constraint, as defined by Zimmermann in a previous study [13]. Single end (double end) arrows denote translational (rotational) constraints. Preliminary studies showed that residual stresses generated using the different boundary conditions do not differ markedly.
Stress peening was simulated using the symmetry cell constraint. Pre-stress is applied by releasing the lateral constraint and imposing a pre-defined displacement in x-direction. By this means, tensile pre-stress prior to shot peening is imposed. After the peening step, the displacement is fully reversed. One must bear in mind that full strain reversal is a condition never reached in reality. Yet, it is assumed to be adequate for basic numerical analyses.

Double peening was carried out using two subsequent shot peening steps. Warm peening was simulated by applying an adequate initial temperature condition to the model.
The chosen material model is based on the approach of Voyiadjis & Abed [6] and described in more detail in the work of Klemenz et al. [7]. It makes use of combined kinematic and isotropic hardening. The yield condition reads

$$f \equiv J_2(\boldsymbol{\sigma}' - \boldsymbol{\xi}) - \sigma_G - R - \sigma^*(T, \dot{\varepsilon})$$

where R and ξ (composed of 2 non-linear variables) denote the scalar isotropic hardening variable and the backstress tensor, respectively. σ_G is the athermal flow stress part of the material. It is temperature dependent only in terms of the shear modulus and independent from strain rate. The thermal flow stress σ* depends on plastic strain-rate $\dot{\varepsilon}^{pl}$ and temperature T. It is given by the equation

$$\sigma^* = \sigma_0^* \left(1 - \left(\frac{k_b T \ln\left(\frac{\dot{\varepsilon}_0}{\dot{\varepsilon}^{pl}}\right)}{\Delta G_0} \right)^n \right)^m$$

where k is Boltzmann's constant and ΔG_0, σ_0^*, $\dot{\varepsilon}_0$, m and n are parameters which have to be determined experimentally.
Push-pull tests at room temperature and low and high speed tensile tests at varying temperatures were carried out to calibrate the material model. The results of those tests and the model parameters derived hereby are shown in Figure 2 and Table 1, respectively.

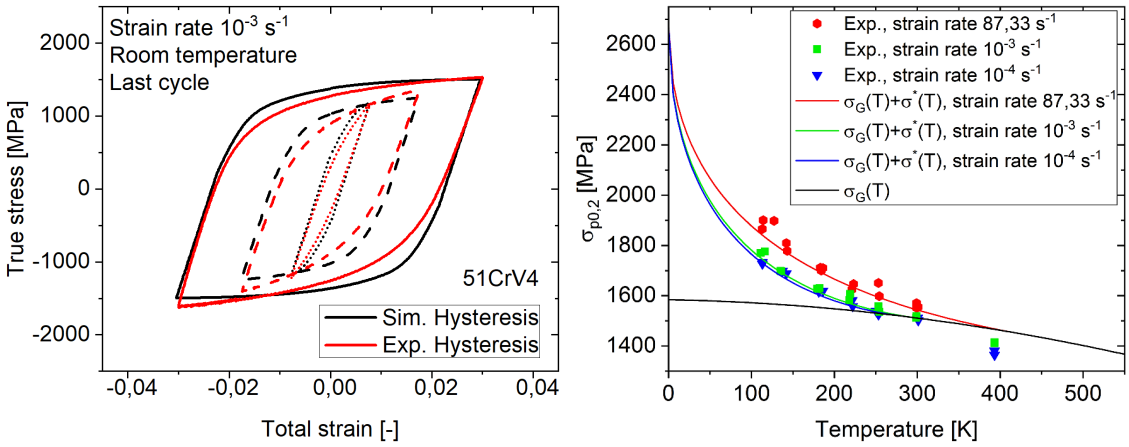

Figure 2. Results of push-pull test (left) and thermal activation model fit (right).

Table 1. Parameters derived for simulation of shot peening variants.

$\sigma_{G,0}$ (σ_G at RT)	ΔG_0	σ_0^*	$\dot{\varepsilon}_0$	m	n
1522 MPa	1.59e-19 J	1088 MPa	5.91e13 s^{-1}	0.5	1.91

Q_1	b_1	C_1	γ_1	C_2	γ_2
-277 MPa	6.93	263050.7 MPa	716.9	24323.3 MPa	83.6

Due to its suitability for nonlinear, dynamic problems, the commercially available equation solver Abaqus/Explicit was used for stress computation. Material data were provided by means of a user material file (VUMAT).
To achieve statistically robust values of residual stresses and field variables after shot peening, an averaging strategy [7] was applied to evaluate the results.

Simulation Results
Figure 3 shows the predicted residual stress states in x-direction after warm peening with different temperatures with (left) and without (right) strain rate dependence of flow stress. In both cases, the simulation predicts lower residual stress magnitudes and higher penetration

depths with increasing process temperature. It becomes obvious that at lower peening temperatures the influence of strain rate is more pronounced. For the simulation, 600 randomly distributed S330-sized shots with a speed of 20 m/s on a surface of 2*2 mm^2 (25% of total model surface) were assumed. This corresponds to a treatment with rather low Almen intensity and high coverage. To achieve absolute comparability of results, shot distribution and shot order were coincident throughout the simulations.

Figure 4 shows the predicted residual stress states after conventional stress peening at 20 °C (top) and warm stress peening at 300 °C (bottom). On the left (right) side, the stress component in x- (y-) direction is shown. For the simulation, 120 randomly distributed S330-sized shots with a speed of 40 m/s on a surface of 2*2 mm^2 (25% of total model surface) were assumed. This corresponds to a treatment with medium Almen intensity and medium coverage (see for instance the investigations of Tange and Ando [9] and Miao et al. [12] for comparison). The tensile pre-stress in x-direction was varied between 0 and 1200 MPa. With increasing pre-stress, both maximum amount and penetration depth of residual stress in x-direction are increased, while the stress in y-direction is not strongly affected. Regarding temperature, the same tendencies as pointed out before prevail.

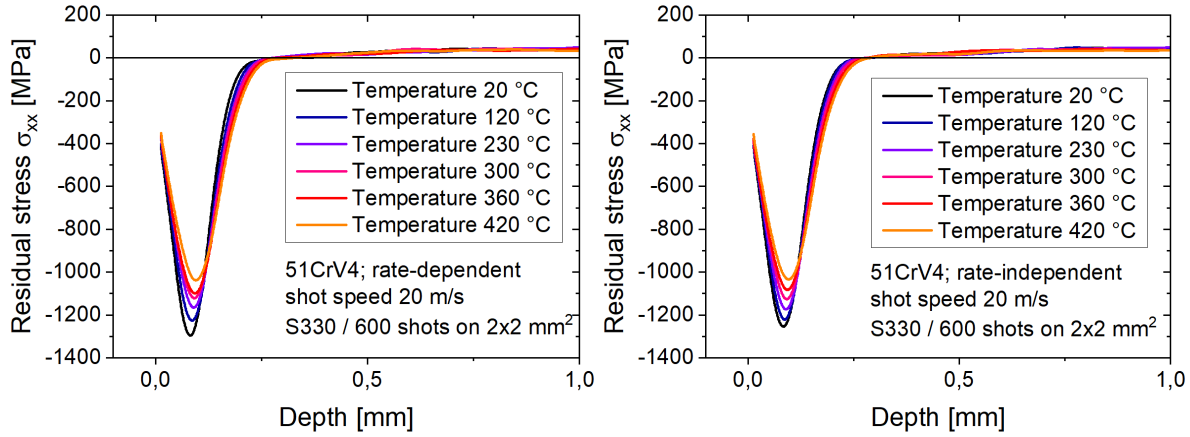

Figure 3. Predicted residual stress profiles after warm peening with (left) and without strain rate dependent material definition (right).

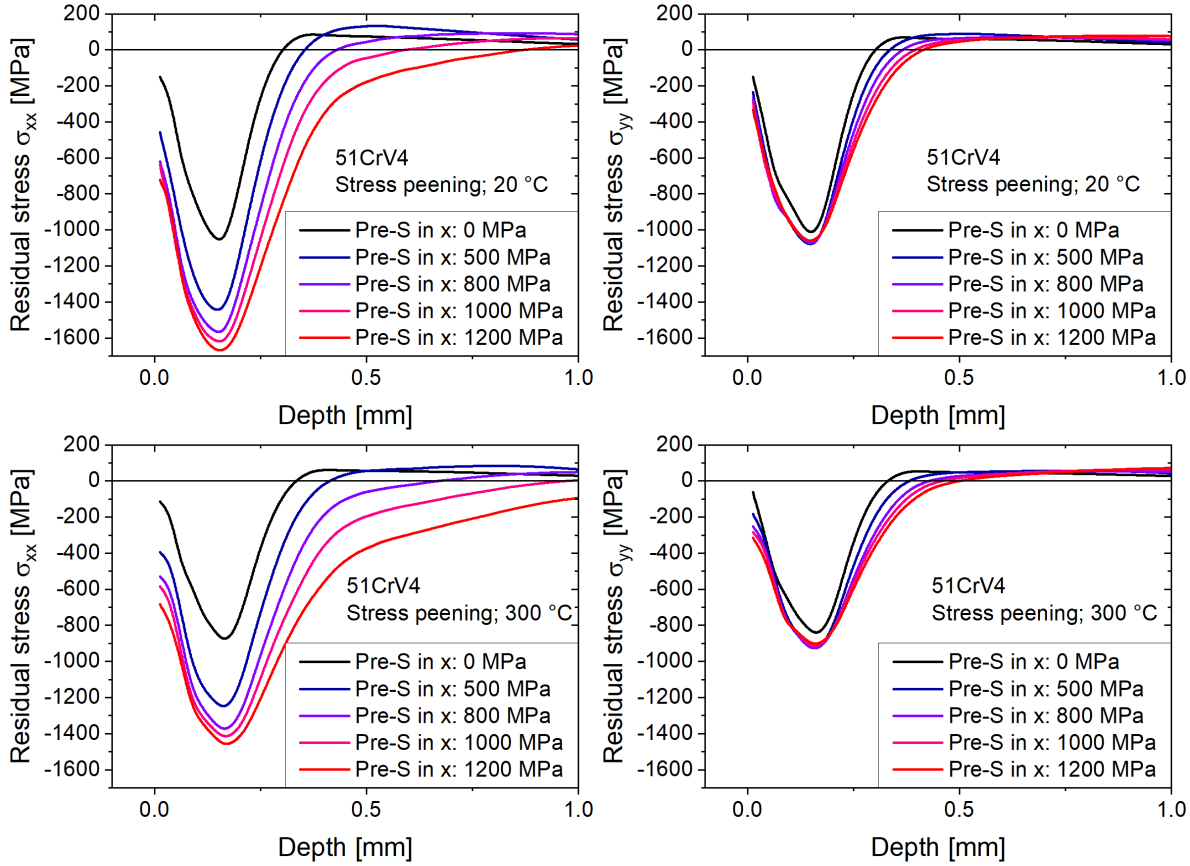

Figure 4. Predicted residual stress profiles after stress peening; top: 20 °C; bottom: 300 °C; left: stress component in x; right: stress component in y.

In Figure 5, the residual stress states after single and double warm peening without pre-stress at 360°C are shown. For the first peening step, 120 randomly distributed S330 shots with a speed of 20 m/s on a surface of 2*2 mm^2 (25% of total model surface) were assumed. For the second peening step, 500 randomly distributed S170 shots were assumed. Shot velocity was varied between 40 m/s and 80 m/s. Obviously, the second shot peening step significantly decreases the near-surface residual stress, while the sub-surface stresses are rather unaffected. This is particularly pronounced for the higher shot velocity.

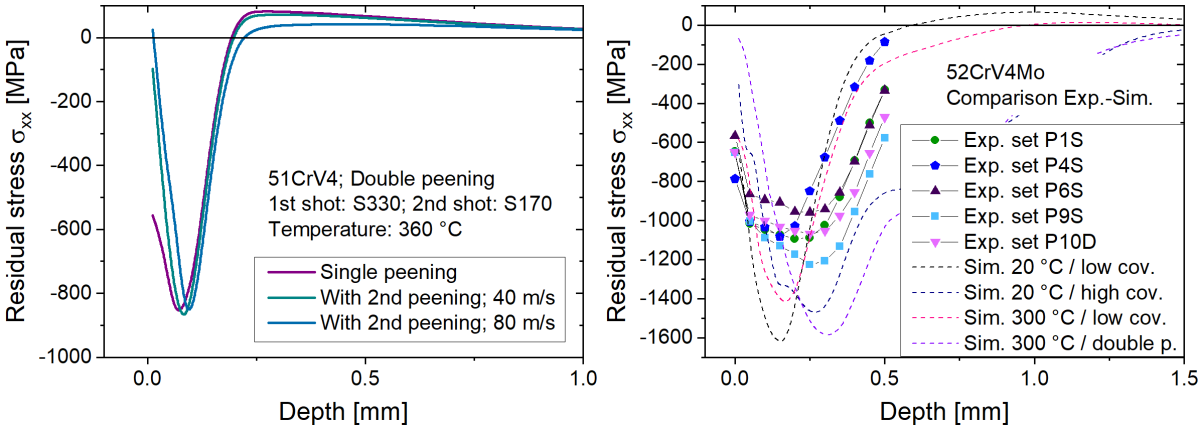

Figure 5. Predicted residual stress states after double peening (left) and comparison with stress peening experimental results (right).

Finally, Figure 5 (right) shows the comparison of numerical with experimental data. Experimental residual stress profiles were derived by stress peening in tension with the procedure described in more detail in [11]. The nomination of parameter sets corresponds to [10]: P1S (standard); P4S (low intensity); P6S (high intensity); P9S (warm); P10D (double).

Experimental stress peening was carried out by shot peening specimens from both sides. It can be seen that despite the fair reproduction of residual stress penetration depth at room temperature, residual stress maxima are largely overestimated.

Discussion and Conclusions

In this study, attention was devoted to the performance of a micro simulation model of conventional shot peening, warm peening and modified stress peening treatments. Besides comparisons of numerical and experimental data, a thorough analysis of the overall predictability of temperature-dependent residual stress formation was carried out. This is necessary since predicted residual stress states markedly depend on model assumptions, particularly regarding material behavior. In this context, Rouhaud et al. [14] compared residual stress prediction with kinematic and isotropic hardening models and showed that a marked influence of the hardening definition exists. Meguid et al. [4] deduced from their investigation on the use of strain-rate dependent flow stress formulation that the definition of the material itself has the strongest influence on the resulting residual stress. Using strain-rate dependent formulations, higher strain rates increase maximum residual stresses and decrease the penetration depth. The same effect prevails using temperature-dependent material data and has experimentally been observed [10,15]. As temperatures are increased, residual stress maxima are reduced and residual stress penetration depths increased. Aside from material definition, the assumption of rigid shots might be questionable when hard targets are treated. Mori et al. [16] deduced from their study that for a yield strength ratio of >2 no plastic deformation of the shot occurs. From target and shot materials used in this study, a yield stress ratio of approx. 2000 MPa / 1600 MPa (56 HRC / 47 HRC) is estimated. Therefore, the assumption of rigid shot in simulations may be a strong overestimation. Rigid shots, in combination with the “hard” strain reversal boundary condition, are expected to yield the strong overestimation of residual stresses after stress-peening, as shown in Figure 5 (right). Regarding double peening, Tange and Ando [9] found beneficially increased surface residual stresses after warm stress double peening. In contrast, decreasing surface residual stresses are predicted by our simulation, as localized deformation – combined with the isotropic softening assumption – softens the material. Yet, strain softening due to shot peening was also observed experimentally and characterized in terms of reduced full width at half maximum values of XRD peaks [10,11].

In summary, strain-rate and temperature dependent material behavior assumptions are an adequate means to predict tendencies in warm peening and warm stress peening. However, other process assumptions regarding the shot and the stress peening conditions might be inadequate and require more realistic modeling. Future studies should thus focus on such process-related assumptions and potential interactions with the material model definition.

Acknowledgement

The authors gratefully acknowledge the financial support of the Research Fund for Coal and Steel under Grant Agreement number: 747346 — LEAFSLIM — RFCS-2016.

References

[1] M. Zimmermann, et al., *Literature review on shot peening simulation*, Int. J. of Computational Materials Science and Surface Engineering 3.4 (2010), pp 289-310.

[2] J. S. Chen, et al., *Literature review of numerical simulation and optimisation of the shot peening process*, Advances in Mechanical Engineering 11.3 (2019), pp 1-19.

[3] A. Gariépy, et al., *Simulation of the shot peening process with variable shot diameters and impacting velocities*, Advances in Engineering Software 114 (2017), pp 121-133.

[4] S. A. Meguid, et al., *3D FE analysis of peening of strain-rate sensitive materials using multiple impingement model*, Int. J. of Impact Engineering 27.2 (2002), pp 119-134.

[5] R. W. Armstrong and S. M. Walley, *High strain rate properties of metals and alloys*, International Materials Reviews 53.3 (2008), pp 105-128.

[6] G. Z. Voyiadjis and F.H. Abed, *A coupled temperature and strain rate dependent yield function for dynamic deformations of bcc metals*, International Journal of Plasticity 22.8 (2006), pp 1398-1431.
[7] M. Klemenz, et al., *Application of the FEM for the prediction of the surface layer characteristics after shot peening*, Journal of Materials Processing Technology 209.8 (2009), pp 4093-4102.
[8] V. Schulze, *Modern mechanical surface treatment: states, stability, effects,* John Wiley & Sons, 2006.
[9] A. Tange and K. Ando, *Improvement of spring fatigue strength by new warm stress double shot peening process*, Materials science and technology 18.6 (2002), pp 642-648.
[10] A. Klumpp, et al., *Experimental Assessment of the Effects of modified Stress Peening Treatments on Surface Layer States and Fatigue Behavior in Leaf Spring Steel 52CrV4Mo*, submitted to Proc. ICSP 14 (2022).
[11] A. Klumpp, et al., *Effects of Shot Peening on Surface Layer States and Fatigue Behavior in Experimental Casts of Enhanced Leaf Spring Steels*, submitted to Proc. ICSP 14 (2022).
[12] H. Y. Miao, et al., *An analytical approach to relate shot peening parameters to Almen intensity*, Surface and Coatings Technology 205.7 (2010), pp 2055-2066.
[13] M. Zimmermann, *Numerische und experimentelle Untersuchungen zur Randschicht-ausbildung beim Druckluft- und Ultraschallkugelstrahlen von IN718*, PhD thesis, Universität Karlsruhe, 2009.
[14] E. Rouhaud, et al., *Finite elements model of shot peening, effects of constitutive laws of the material*, Proc. ICSP 9 (2005), pp 107-112.
[15] Y. Harada and K. Mori, *Effect of processing temperature on warm shot peening of spring steel*, Journal of Materials Processing Technology 162 (2005), pp 498-503.
[16] K. Mori, et al., *Rigid-plastic finite element simulation of peening process with plastically deforming shot*, JSME international journal. Ser. A, Mechanics and material engineering 39.3 (1996), pp 306-312.